IEEE Photonics Journal
An IEEE Photonics Society Publication

Open Access

Nearly Degenerate Four-Wave Mixing in Single-Mode Fabry–Pérot Laser Diode Subject to Single Beam Optical Injection

Volume 9, Number 1, February 2017

Jian-Wei Wu
Yong Hyub Won

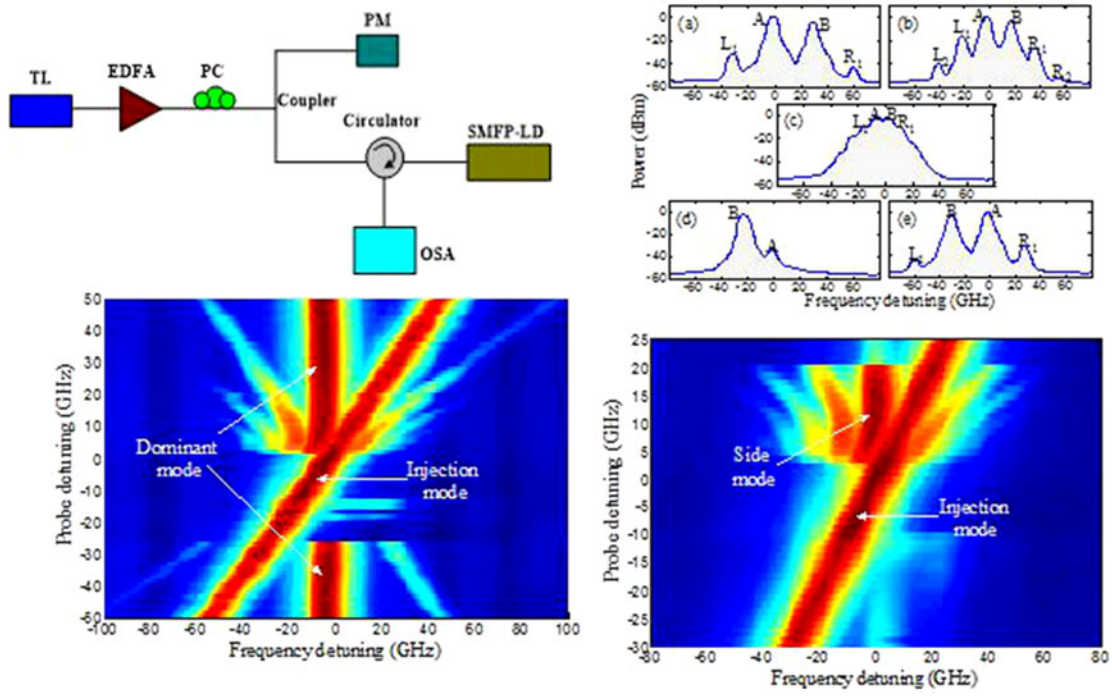

DOI: 10.1109/JPHOT.2016.2636744
1943-0655 © 2016 IEEE

Nearly Degenerate Four-Wave Mixing in Single-Mode Fabry–Pérot Laser Diode Subject to Single Beam Optical Injection

Jian-Wei Wu[1] **and Yong Hyub Won**[2]

[1]College of Physics and Electronic Engineering, Chongqing Normal University
Chongqing 401331, China
[2]School of Electrical Engineering, Korea Advanced Institute of Science and Technology,
Daejeon 34141, South Korea

DOI:10.1109/JPHOT.2016.2636744

Manuscript received June 30, 2016; revised November 4, 2016; accepted December 2, 2016. Date of publication December 7, 2016; date of current version December 21, 2016. This work was supported in part by the National Natural Science Foundation of China under Grant 61205111; in part by the Open Foundation of State Key Laboratory of Millimeter Waves under Grant K201513; in part by the Open Foundation of State Key Laboratory of Advanced Optical Communication Systems and Networks, China; in part by the China Postdoctoral Science Foundation under Grant 2014M562293; in part by the West Project of China Scholarship Council under Grant 201408505054 and in part by the Open Foundation of State Key Laboratory on Integrated Optoelectronics under Grant IOSKL2016KF02. Corresponding authors: J.-W. Wu (e-mail: jwwu@uestc.edu.cn).

Abstract: In this paper, nearly degenerate four-wave mixing created by pump–probe structure with small frequency spacing and enough high power is demonstrated and discussed by introducing single optical beam into single-mode Fabry–Pérot laser diode, in which the injected beam is called the probe wave, whose frequency detuning is controlled within ±50 GHz, and lasing resonance mode such as dominant mode or arbitrarily residual side mode is selected as the pump wave. In the case of dominant mode like the pump wave, conjugate signals around the pump–probe wave are easily observed for positive and negative probe detuning by judiciously tuning injected probe power. While external injection mode is moved towards the side mode selected as the pump wave, newly generated signals only occurred with small positive probe detuning. As the probe wave with positive frequency detuning is close to the pump wave, higher order conjugate signals are gradually grown. Under the condition of side mode as the pump wave, the strongly nonlinear mixing of the pump–probe wave also gives rise to new frequency signals on both sides of the dominant mode with enough high peak level. Against the change of correspondingly initial power and frequency detuning of the probe wave, outcome spectrum, output power, and conversion efficiency of conjugate signals are analyzed in detail, while dominant or one side mode is, respectively, selected as the pump wave.

Index Terms: Nonlinear optics, single mode semiconductor laser, optical injection, nearly degenerate four-wave mixing.

1. Introduction

Over the past few decades, four-wave mixing (FWM) as an important nonlinear process has been attracted intensive attention in various optical materials [1]–[6] and are successfully applied in various all-optical functions such as wavelength conversion [7], [8], switching [9], parametric oscillator [10], logic gate [11], [12], sensor [13], modulation [14], and other technologies [15]–[18], owing

to its significant advantages such as high operation speed, broadly tunable range, multiple signal conversion, and transparent operation.

As compared to other medias, semiconductor that has high nonlinear effects and potentially compact scale has been extensively adopted to present some optical devices including lasers [19], [20], waveguides [21], [22], and amplifiers [23], [24], in which strong nonlinear FWM phenomenon can be observed by judiciously adjusting powers and wavelengths of external injection beams. In general, based on different beat frequencies between two injected beams, both highly non-degenerate and nearly degenerate FWM are demonstrated and discussed in previously semiconductor based reports, and have some advanced applications for all-optical signal processing techniques such as mode-selective wavelength conversion, microwave and millimeter wave generation given in recent demonstrations [25], [26]. Undoubtedly, various semiconductor lasers in the semiconductor family play prominent roles for achieving four-wave mixing related technologies, which bring some significant applications and strongly competitive abilities in recent years. Even so, the presented semiconductor lasers such as quantum-dot laser and multimode laser have some strict limitations including high cost, or low side-mode suppression ratio (SMSR). Therefore, to overcome these disadvantage factors of some semiconductor lasers, a novel single-mode Fabry-Pérot laser diode (SMFP-LD) that has some prominent properties including simple structure, broadly tunable range, high SMSR, cost effective, self-locking resulting from its special structure is presented and demonstrated in recent years. SMFP-LD is fabricated by using the well-known multimode quantum well semiconductor laser with a built-in external cavity [27], and has more compact scale compared to other wavelength selectable laser with external cavity feedback [28]. Through a great deal of experimental investigations, one can find that SMFP-LD exhibits attractive characteristics in wavelength conversion [29], modulation [30], logic gate [31], photonic generation [32], and optical memory [33] by means of external optical injection or feedback beam. In recent research, the highly nondegenerate FWM phenomenon in SMFP-LD was reported by using two external injection beams, and takes on some interesting behaviors owing to special design structure of laser [34]. In the case of highly nondegenerate FWM, all of lasing resonance modes including dominant and side modes should be thoroughly suppressed by the external injection modes in order to suppress noise and clearly display newly generated conjugate signals.

In order to further explore the FWM effect in SMFP-LD, the nearly degenerate FWM process is presented and researched in this work, in which an external injection mode as the probe wave combined with dominant mode or side mode as pump wave gives rise to nearly degenerate FWM interaction. Compared to the case of highly nondegenerate FWM with up to 100 GHz pump-probe detuning, the frequency interval between pump and probe waves for nearly degenerate FWM ranges from a few GHz to several tens of GHz so that powers of conjugate signals are significantly enhanced, and cascade FWM interactions are easily observed owing to enhanced wave mixing process. In reality, nearly degenerate FWM has already mentioned by using other semiconductor laser [26], [35], [36], and amplifier [37] subject to external injection beams. Generally, more complicated structures are requested to perform the nearly degenerated FWM process in previous reports. Nevertheless, it is surprising that nearly degenerate FWM process given in this study can be easily achieved by only injecting an external injection mode into SMFP-LD so that the experimental setup is simplified, and both injection and side modes can also produce effectively FWM interaction. The achieved output power and conversion efficiency (CE) for generated FWM-signals are strongly dependent on injection power and frequency detuning of probe wave. Through this work, one can believe that SMFP-LD based nearly degenerate FWM will open up some potential applications such as optical sensor, low frequency microwave, and millimeter wave signal generation, which will be demonstrated in future investigations.

2. Experimental Setup and Operation Principle

Fig. 1 shows the schematic diagram of experimental setup to perform nearly degenerate FWM process. By adjusting the bias current and operation temperature of SMFP-LD, it can emit single mode optical spectrum, in which the power of dominant mode is remarkably higher than those at

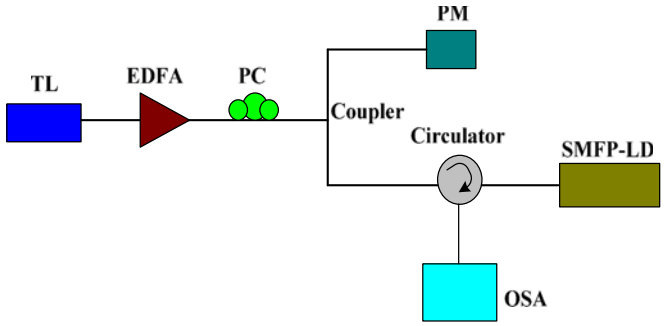

Fig. 1. Experimental setup. TL: Tunable laser, EDFA: Erbium-doped fiber amplifier, PC: Polarization controller, PM: Power meter, OSA: Optical spectrum analyzer.

other residual side modes. So, the resulted output spectrum has as high as over 30 dB SMSR and about 10 nm dynamically tunable range for wavelength of dominant mode by selecting various working currents and temperatures in active media. The details of SMFP-LD design can be known in [27], in which more properties of output spectrum can be got.

In experiment, the dominant mode or other arbitrarily side mode in the output spectrum of SMFP-LD is, respectively, selected as the pump wave during performing nearly degenerate FWM, in which the external continuous wave emitted by the external tunable laser (TL) is called as probe beam, whose injection power can be enhanced or decayed by flexibly controlling gain level of erbium-doped fiber amplifier (EDFA). The polarization state of output beam from EDFA is tuned to TE wave same as dominant mode via polarization controller (PC) to guarantee effective FWM interaction. Here, PC can also suppress the noise created by EDFA. Then, the probe wave with TE state is divided into two branches by the 50/50 fiber directional coupler. Half port is connected to a power meter (PM) to indirectly monitor the injection power of SMFP-LD, whereas the remained half branch is injected into the SMFP-LD via the optical circulator with 3 dB loss. As a consequence, nearly degenerate FWM produced by nonlinear interaction of pump and probe waves in active media can be occurred by judiciously selecting input power and frequency detuning of injected probe wave. Here, the frequency detuning is defined as the frequency difference between frequency of injected wave (or frequencies of output spectrum) and frequency of the referred dominant mode or side mode in free-running spectrum from SMFP-LD. Positive (negative) probe detuning denotes that the frequency at probe mode is larger (smaller) than that of the corresponding pump mode, and can be slowly adjusted to observe nearly degenerate FWM interaction. Here, it should be pointed out that, while the frequency detuning of probe wave is held a very small constant, the frequency spacing of output pump-probe wave shown in OSA has fluctuation attributed to strong field interaction with respect to the changes of input power of probe wave. Here, the frequency spacing of both output pump and output probe waves is defined as pump-probe detuning whose value has some difference with the given probe detuning in the cases of very small intervals between pump and probe waves. On the other hand, one can also find in the experiment that the defined frequency detuning of probe wave is nearly equal to the frequency difference between output pump and probe waves for larger separations of pump-probe wave. Via circulator, the output spectrum from SMFP-LD can be captured by the optical spectrum analyzer (OSA), in which the beat frequency of output pump and probe waves, and peak power of each output signal can be directly measured. Based on injection power of probe wave and output powers of conjugate signals, FWM conversion efficiency for each new signal can be obtained by means of calculation, and is strongly related to the pump-probe detuning and injected probe power.

3. Results and Discussion

Four-wave mixing as a well-known nonlinear parametric process is driven by third-order nonlinear susceptibility $\chi^{(3)}$. Generally, five kinds of third-order nonlinear processes including carrier-density

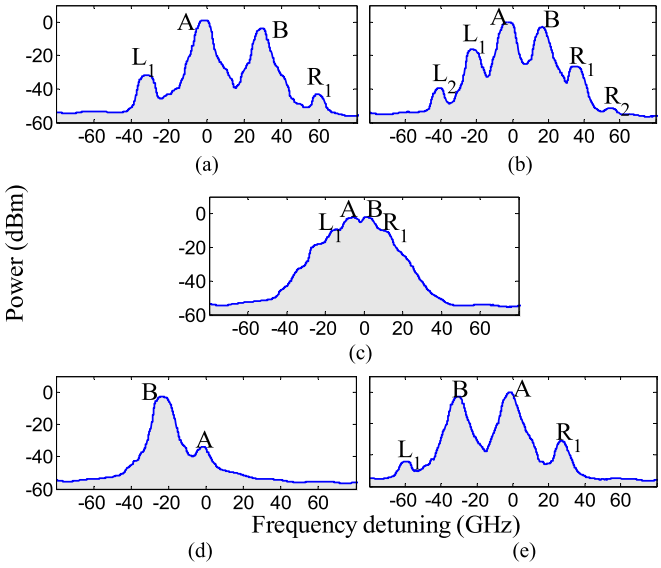

Fig. 2. Output spectra displayed by OSA under the conditions of an external injection mode with −6 dBm input power and various pump-probe detunings. (a) $f_B - f_A = 30$ GHz, (b) $f_B - f_A = 19$ GHz, (c) $f_B - f_A = 7$ GHz, (d)$f_A - f_B = 21$ GHz, and (e) $f_A - f_B = 28$ GHz.

pulsation (CDP), spectral hold burning (SHB), carrier heating (CH), two-photon absorption (TPA), and the Kerr effect contribute to the four-wave interaction in semiconductor materials, in which the gain and refractive index of active region are modulated by the beat frequency of pump-probe wave, leading to moving gain and index gratings that will diffract the input fields to generate additional FWM-signals. However, in the case of less than 8 THz pump-probe detuning, influences of both TPA and Kerr effects on the FWM process can be ignored, i.e., CDP, SHB, and CH will, respectively, dominate the nonlinear parametric dynamic at different pump-probe detunings, in which, for less than 100 GHz detuning, both SHB and CH can be safely neglected, and only nonlinear interband process, CDP, plays an important role in nearly degenerate FWM within less than ±50 GHz probe detuning in the following discussion [38], [39].

In the case of bias current of 28 mA and operation temperature of 24.2 °C for SMFP-LD, the dominant mode of output free-running spectrum is locked at 194.387 THz frequency. Output spectra of nearly degenerate FWM with various pump-probe detunings are plotted in Fig. 2, where the dominant mode denoted by A is selected as the pump wave, and the external injection mode with −6 dBm input power is called as the probe wave labeled as B that is gradually shifted from one side to another side of dominant mode. The horizontal axis denotes the frequency detuning between output spectrum and dominant mode of free-running spectrum. As indicated in these spectra, strong nearly degenerate FWM process is achieved for some special frequency detunings. Both of frequencies of pump and probe waves are given by f_A and f_B so as to the absolute pump-probe detuning $\Omega = |f_A - f_B|$. The carrier density in active media is modulated by the beating of pump and probe fields at the beat frequency Ω so that the dynamical gain and index gratings are formed in the gain region. And then, both pump and probe beams are, respectively, diffracted by the moving gratings to generate fundamental order conjugate signals at $f_A - \Omega$, $f_A + \Omega$, $f_B - \Omega$ and $f_B + \Omega$ frequencies [39]. In Fig. 2(a), where the pump-probe detuning is 30 GHz, and seeable conjugate signal on OSA for pump (probe) wave is located at $f_A - \Omega$ ($f_B + \Omega$) frequency. As the corresponding pump-probe detuning is reduced to 19 GHz given in Fig. 2(b), higher order FWM signals (L_2 and R_2) generated by nonlinear interaction of low order conjugate signals (L_1 and R_1) and pump-probe beam are gradually grown. Owing to small detuning, the powers of signal L_1 and R_1 are significantly enhanced compared to the case of 30 GHz detuning. As such, the direct result of enhanced conjugate signal L_1 and R_1 is to induce the generation of higher order conjugate signal

L_2 and R_2 [1], [40]. In Fig. 2(c) with 7 GHz pump-probe detuning, it is difficult to distinguish newly generated signals, especially for higher order conjugate signals, and peak levels of signal L_1 and R_1 are further increased. Here, both of output peaks for pump and probe waves have almost equal levels due to their nonlinear overlapping. As can be seen in Fig. 2(d), the pump-probe detuning is again extended to 21 GHz, in which, however, the probe wave is positioned on left side of pump beam, i.e., negative probe detuning. It is surprising that the pump mode is remarkably suppressed resulting from injection locking and strong free carrier absorption of probe beam, in which the injected probe with enough high power absorbs a great deal of free carrier of active region due to stimulated emission process so that the power at dominant mode is rapidly dropped as a result of the reduced free carrier density. Consequently, emission mode of output spectrum is shifted to injection mode. However, in Fig. 2(d), the dominant mode still exhibits one peak with very low power value compared to that of injection mode, and isn't fully suppressed because the power of injection mode is not too high under the determined probe detuning condition, namely, the injection locking in SMFP-LD is directly dependent on the power and frequency detuning of injection mode. Therefore, it is easily understood that, by further increasing the injected probe power, the dominant mode can be thoroughly suppressed with the result that the emission mode is locked to probe frequency. Because of large power difference of pump and probe waves caused by too low pump power, the nonlinear FWM interaction is disappeared in Fig. 2(d). Obviously, as the injected probe wave is far from the dominant mode so as to be outside injection locking range, the power of dominant mode again jumps back to comparable level to the case in free-running spectrum. This result is shown in Fig. 2(e), in which the pump-probe detuning is increased to 28 GHz. As a consequence, the nearly degenerate FWM interaction is again displayed, resulting in generating newly conjugate signals L_1 and R_1 around the pump-probe beam. Here, it should be noted that, in the cases of positive probe detunings, e.g. in Fig. 2(b) and (c) with very small pump-probe detuning, the injected wave with properly high power can also make other side modes, except dominant mode, to be suppressed resulting from strongly stimulated emission of pump and probe waves. Additionally, through experiment in positive probe detuning, one can find that the other suppressed side modes have no any frequency shift that should be distinguished to the case of negative frequency detuning. These corresponding results aren't detailedly given in this study. But, one can find that the peak position of dominant mode has some shift because of strongly nonlinear interaction between pump and probe modes in the small pump-probe detunings, as shown in Fig. 2(b) and (c).

To more clearly characterize the output spectrum of nearly degenerate FWM, Fig. 3(a)–(c) with incident power set to -4.6 dBm plot, respectively, the outcome spectral evolutions, output powers, and conversion efficiencies with respect to the probe detuning, ranging from -50 GHz to 50 GHz. In Fig. 3(a), one can see that the optical phenomena created by nonlinear interaction of pump-probe beam are strongly dependent on probe detuning, in which, as it is shifted from ~ -25 GHz to ~ 0 GHz, the primary dominant mode is disappeared as a result of the locking behavior caused by injected probe beam. This behavior can be explained that, while the probe wavelength is slightly longer than that of dominant mode, the refractive index of active region is increased due to the reduced free carrier density caused by the enhanced stimulation emission of probe wave. Hence, the enhanced refractive index leads to redshift of the corresponding lasing mode, and makes the output spectrum lock to probe wavelength. As a result, one cannot observe the FWM process, and output peak of probe wave can reach maximum power level shown in Fig. 3(b). During ~ -25 GHz to -50 GHz probe detuning, the dominant mode is again occurred resulting in producing nearly degenerate FWM that is always occurred as the probe detuning is continuously changed from ~ 0 GHz to 50 GHz. But, in the case of less than ~ 20 GHz detuning, it is easy to achieve higher order conjugate signals on both sides of pump-probe wave. While the referred frequency detuning is extended to up to ~ 20 GHz, only fundamental order FWM signals are generated. The obtained power for each conjugate signal clearly illustrated in Fig. 3(b) is gradually decayed with absolute probe detuning increase, and can reach maximum power level at about 5 GHz frequency detuning and is slightly dropped because of the enhanced stimulated emission for pump-probe beam at less than 5 GHz detuning, in which other higher order signals cannot be easily observed due to the combined limitations of lasing mode linewidth and OSA resolution. Therefore, while the probe

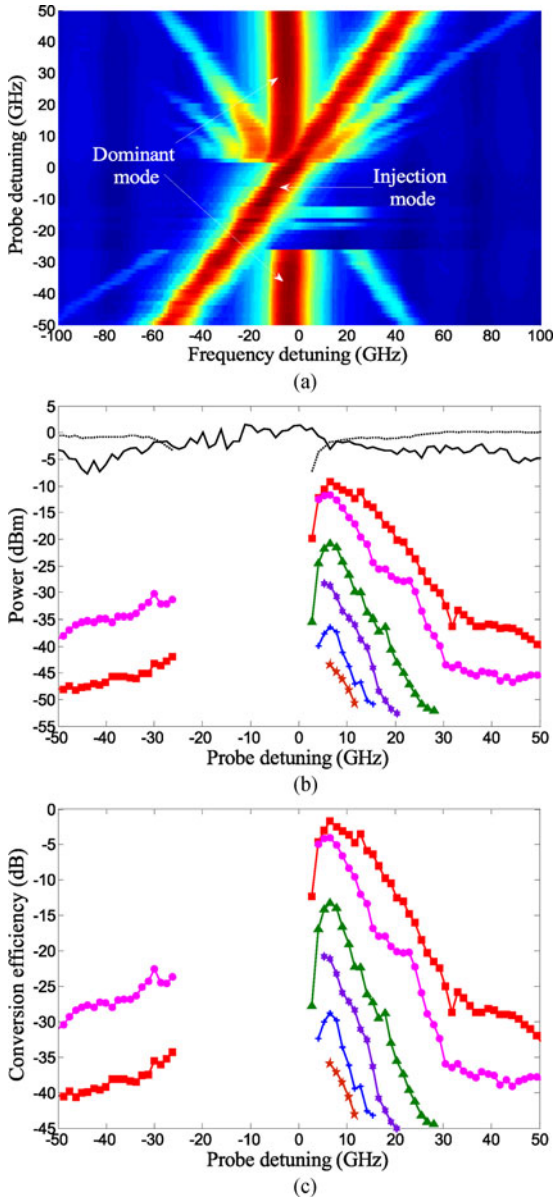

Fig. 3. Against changed probe detuning. (a) Evolution of output spectrum. (b) Output peaks of pump wave, probe wave, and conjugate signals. Black solid line stands for probe wave, and the black dotted line stands for pump wave. (c) Conversion efficiencies for newly generated FWM-signals. Red lines with closed square marks stand for signal L_1, pink lines with closed circular marks for signal R_1, green line with closed triangle marks for signal L_2, purple line with closed six-pointed star marks for R_2, blue line with cross marks for L_3, and brown line with closed pentagram marks for R_3.

detuning is varied from 5 GHz to 10 GHz, the first, second, and third order conjugate signals are, respectively, shown around pump and probe waves because of the enhanced FWM interaction in small detuning range. Conversion efficiency defined by the ratio of conjugate signal power to the incident probe power is an important parameter to assess FWM effect [41] and is plotted against the probe detuning in Fig. 3(c), where the variable trend of CE is same as the power case shown in Fig. 3(b), and the maximum CE can be close to 0 dB that is higher than most reported cases [42], [43]. Additionally, while the frequency detuning of probe wave is held a constant, the CE of low order FWM signal is higher than that of higher order signal. Therefore, it is obvious that, in

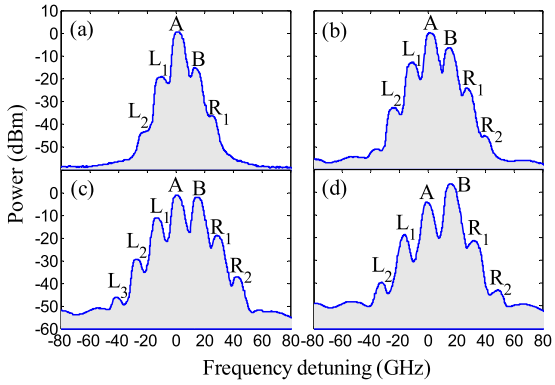

Fig. 4. Output spectra for 12 GHz probe detuning and various injected probe powers. (a) −16 dBm, (b) −8.5 dBm, (c) −3.5 dBm, and (d) 0 dBm.

order to increase the CE, the peak power of output conjugate signal should be enhanced at a fixed input probe power. Actually, the output power or conversion efficiency of conjugate signal in semiconductor laser is strongly dependent on the phase mismatch, gain of active region, and initial power of pump-probe wave. While probe wave is shifted towards pump wave leading to the small pump-probe detuning, the phase mismatch is rapidly reduced, resulting in the enhanced CE and conjugate signal peak shown in Fig. 3(b) and (c) [44]. Contrarily, when the pump-probe detuning is too small, e.g. less than ∼5 GHz, both output power and CE of conjugate signal are slightly decayed as a result of mode competition between original signal and new signal, in which the probe wave with high peak gives rise to gentle power suppression of pump wave and generated FWM signals.

To measure the influence of incident probe power on the nearly degenerate FWM process at a fixed probe detuning, the corresponding output spectra, output power, and conversion efficiency are, respectively, plotted in Fig. 4 to Fig. 7. In Fig. 4 with 12 GHz probe detuning, one can see that various spectra are displayed by respectively selecting different initial probe power of −16 dBm, −8.5 dBm, −3.5 dBm, and 0 dBm. In the case of −16 dBm probe power, three conjugate signals including L_1, L_2, and R_1 are only exhibited in Fig. 4(a). But, as the probe power is increased to −8.5 dBm and −3.5 dBm, at least four or five FWM-signals shown in Fig. 4(b) and (c) are generated owing to the enhanced nonlinear FWM interaction that is the direct result of increased probe power. On the other hand, it is surprising that the generated new frequency signals given in Fig. 4(d) are suppressed at 0 dBm probe power, in which the probe wave will absorb a great deal of free carrier of active region so that the gains of other signals such as pump wave, and FWM-signals are gradually reduced. More detail variations are illustrated in Fig. 5(a) and (b), where both output power and conversion efficiency are plotted as a function of input probe peak, ranging from −16 dBm to 0 dBm. When probe power is varied from ∼−5 dBm to ∼−2 dBm, both of pump and probe waves have comparable peak level, leading to stronger FWM interaction. Consequently, more new frequency signals are grown. In addition, it should be noted that peak of conjugate signal L_1 is always higher than other new signals with the result that the obtained conversion efficiency for L_1 is remarkably larger than those of other signals. The maximum CE of L_1 is around 0 dB for low input probe peak level under the fixed probe detuning of 12 GHz condition.

While probe wave is shifted to left side of pump mode, namely, probe frequency is smaller than that of pump wave, various spectra are given in Fig. 6(a)–(d) with −21 GHz probe detuning and four input power levels. At −5 dBm input probe power, the exhibited spectrum shown in Fig. 6(a) is similar to the case in Fig. 2(d) so that nonlinear FWM effect cannot be observed because of too low peak power for pump beam. As the probe power is decreased to −11.5 dBm level, the pump power is again recovered to enough high level, resulting in generating new FWM-signals, as illustrated in Fig. 6(b). Obviously, when probe power is reduced to −16.5 dBm and −19.5 dBm, respectively, the FWM interaction is slowly weakened with the result that FWM-signals also begin to decay till disappearance. As can be seen in Fig. 7(a) and (b), after the pump beam is fully recovered to

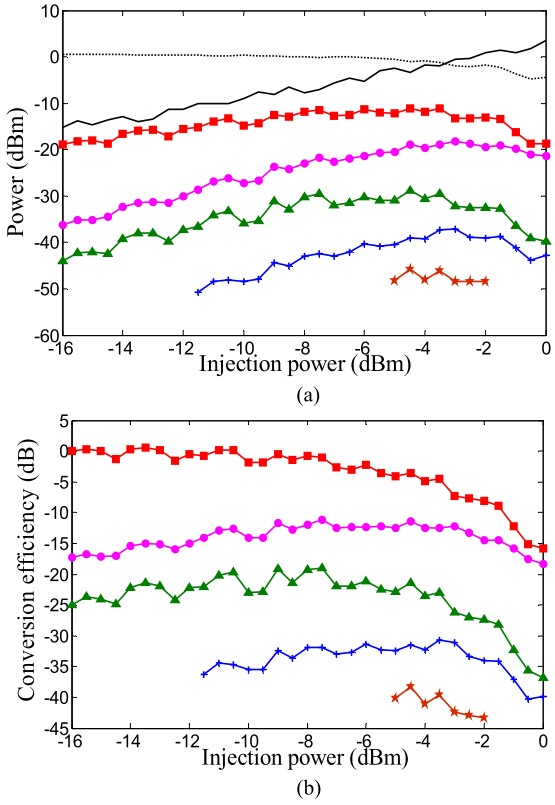

Fig. 5. At 12 GHz probe detuning, with respect to change of injection power for probe wave. (a) Peaks of pump wave, probe wave, and conjugate signals. Black solid line stands for probe wave, and black dotted line for pump wave. (b) Conversion efficiencies for conjugate signals. Red lines with closed square marks stand for signal L_1, pink lines with closed circular marks for signal R_1, green line with closed triangle marks for signal L_2, blue line with cross marks for R_2, and brown line with closed pentagram marks for L_3.

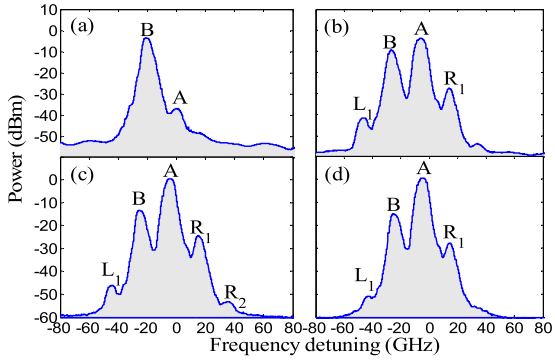

Fig. 6. Output spectra for −21 GHz probe detuning and various injected probe powers. (a) −5 dBm, (b) −11.5 dBm, (c) −16.5 dBm, and (d) −19.5 dBm.

enough high power level under the condition of less than −10 dBm probe power, FWM-signals are generated resulting from beat effect between pump and probe waves. However, it is obvious that, as the probe power is further decayed, resulting in the enlarged power difference of both output pump and probe waves, it is believed that the output power of conjugate signal is gradually reduced till completely disappearance. Based on above discussion, one can conclude that, in the cases of dominant mode as pump wave, and determined bias current and operating temperature for laser,

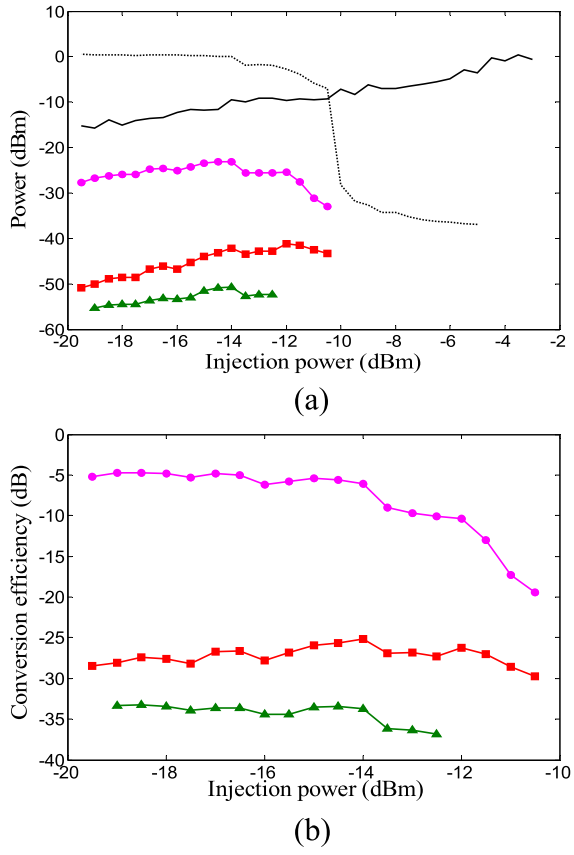

Fig. 7. At −21 GHz probe detuning, with respect to change of injection power for probe wave. (a) Output peaks of pump wave, probe wave, and conjugate signals. Black solid line stands for probe wave, and black dotted line stands for pump wave. (b) Conversion efficiencies for conjugate signals. Red lines with closed square marks stand for signal L_1, pink lines with closed circular marks for signal R_1, and green line with closed triangle marks for signal R_2.

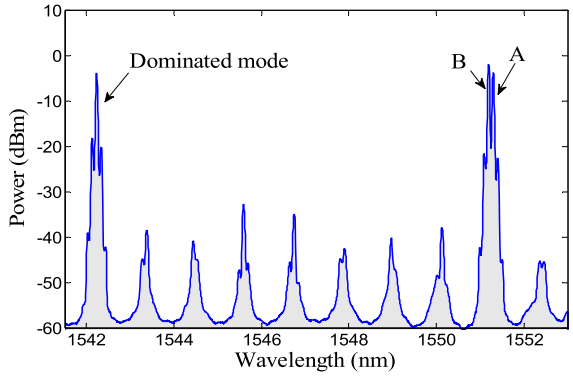

Fig. 8. Output spectrum with side mode as pump wave and −8 dBm injected probe power.

spectral characteristics of nonlinear FWM process such as output power and conversion efficiency are strongly related to probe power and detuning.

Now, let us focus on the case of arbitrarily residual side mode as pump wave, as shown in Fig. 8, in which, based on the outcome spectrum, it can be seen that newly generated signals around the injected wave B and side mode A with enhanced power, owing to nearly degenerate FWM interaction, and the fundamental order signal is shifted from the pump or probe wave by

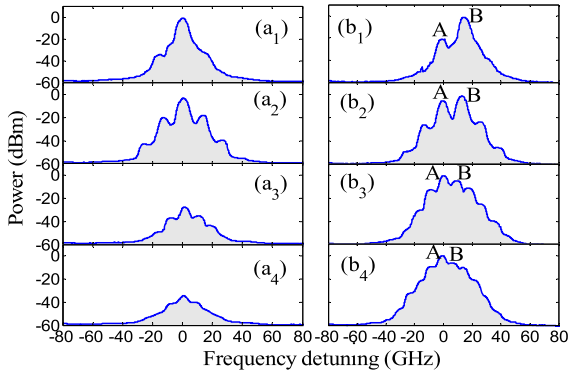

Fig. 9. Output spectra of (a) dominant mode and (b) wave mixing of pump-probe beam with various frequency detunings. b_1: 14 GHz, b_2: 13 GHz, b_3: 9 GHz, and b_4: 6 GHz.

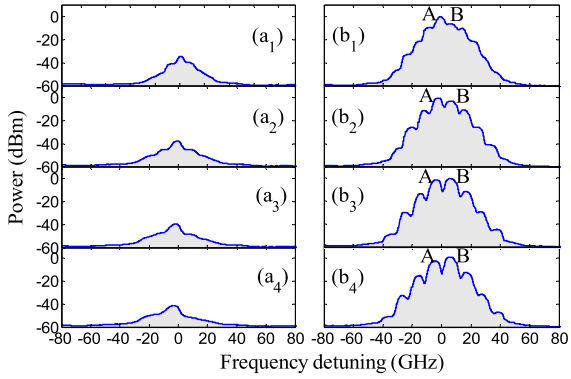

Fig. 10. Output spectra of (a) dominant mode and (b) wave mixing of pump-probe beam with various probe powers. b_1: −8 dBm, b_2: −6 dBm, b_3: −4 dBm, and b_4: −2 dBm.

beat frequency of 13 GHz. In Fig. 8, another interesting phenomenon should be noted that other lasing resonance modes also produce new signals around them, in which these newly generated signals should be the direct result of diffractions of lasing modes by the moving grating induced by pump-probe wave. As such, the frequency spacing of the fundamental order conjugate signal and the corresponding lasing mode is still equal to beat frequency of pump-probe wave. Except for the case of pump-probe beam, the power of other new signals generated by the diffraction of dominant mode and other side mode are strongly dependent on their peak level, i.e., high power is easily to induce generation of new conjugate signals under the effective beating of pump-probe beam condition. Therefore, the dominant mode with higher power than other side mode produces more new frequency signals whose peaks are obviously stronger than those of the corresponding signals around other side modes.

Under the side mode as pump wave the condition, the dependences of characteristics of dominant mode and FWM-spectrum on pump-probe detuning and input probe power are depicted in Fig. 9, where other parameters are same as those in Fig. 8, and the outcome spectra of dominant mode shown in Fig. 9(a_1)–(a_4) are, respectively, displayed as the reduced pump-probe detuning obtained by shifting the probe frequency towards the pump wave. In Fig. 9(b_1) with 14 GHz pump-probe detuning, effective FWM cannot be observed due to low pump power so that the dominant mode still takes on single peak. The pump power is significantly enhanced as the detuning is decreased to 13 GHz shown in Fig. 9(b_2), in which obvious conjugate signals are generated. At present, one can surprisingly find that new conjugate signals are grown around the dominant mode. However, in the cases of both 9 GHz and 6 GHz pump-probe detunings illustrated in Fig. 9(b_3) and (b_4), the power of pump wave, A, is increased as a result of interaction of pump-probe beam. In active gain region, a great deal of free carrier is depleted by the pump-probe wave so that the dominant

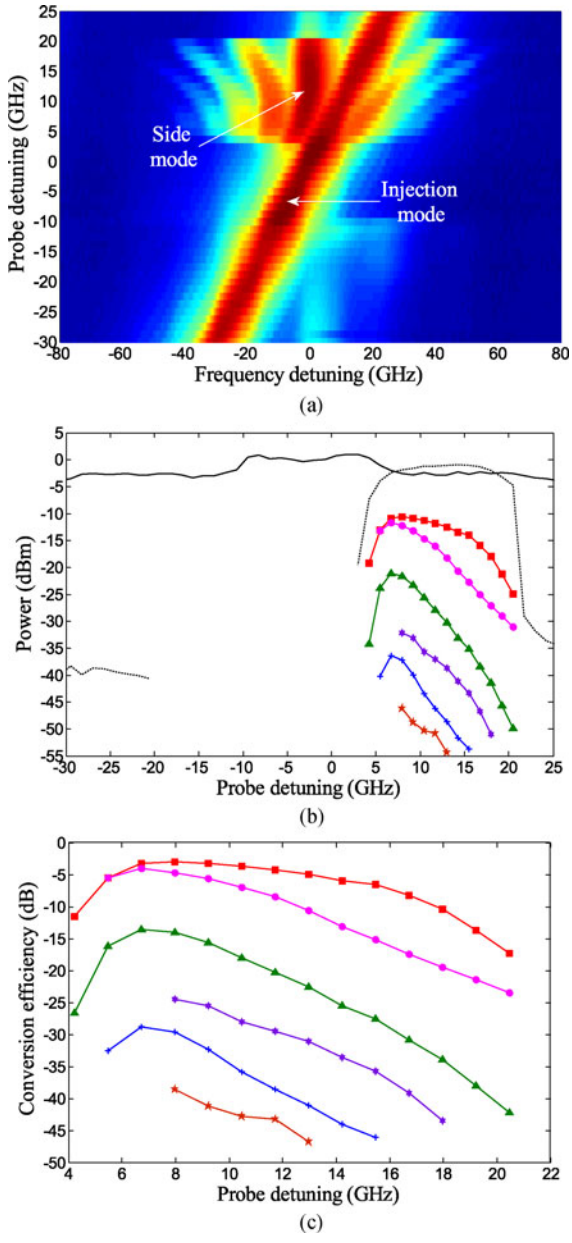

Fig. 11. Against changed frequency detuning between injected probe mode and selected side mode of free-running spectrum. (a) Evolution of output spectrum. (b) Output peaks of pump wave, probe wave, and conjugate signals. Black solid line stands for probe wave, and black dotted line stands for pump wave. (c) Conversion efficiencies for newly generated FWM-signals. Red lines with closed square marks stand for signal L_1, pink lines with closed circular marks for signal R_1, green line with closed triangle marks for signal L_2, purple line with closed six-pointed star marks for R_2, blue line with cross marks for L_3, and brown line with closed pentagram marks for R_3.

mode is strongly suppressed shown in Fig. 9(a_3) and (a_4), in which, without enough high power for dominant mode, it is difficult to generate notable conjugate signals. Additionally, in Fig. 9(b_4), it is difficult to distinguish newly generated FWM-signals resulting from combined limitations of linewidth for pump-probe wave and OSA resolution. Here, by increasing the probe power, dramatic FWM signals around the pump-probe mode are again occurred, which are, respectively, plotted in Fig. 10(b_2)–(b_4) with probe powers of −6 dBm, −4 dBm, and −2 dBm. This behavior can be

explained that, as the probe power is increased from −6 dBm to −2 dBm, the pump-probe detuning of outcome spectrum is slightly extended attributed to their nonlinear interaction, and is, respectively, increased to ∼8.0 GHz, ∼9.7 GHz, and ∼10.1 GHz. As a result, the newly generated conjugate signals are easily observed in the case of an extended pump-probe detuning displayed in Fig. 10. In addition, the corresponding dominant modes shown in Fig. 10(a_1)-(a_4) are always suppressed due to high probe power that causes the laser to lock at pump-probe wavelength with the result that one cannot achieve obvious conjugate signals around the dominant mode.

To compare with the case of Fig. 3, the evolutions such as optical spectrum, output power, and conversion efficiency against the probe detuning are, respectively, displayed in Fig. 11, in which one side mode is selected as pump wave, and the incident probe power is −4.6 dBm that is identical to that in Fig. 3. From Fig. 11(a), it is clearly shown that, as the probe frequency detuning is changed from ∼−30 GHz to ∼25 GHz, the outcome spectrum shows some variously optical properties, compared to those of Fig. 3. Nonlinear FWM process is only occurred in the range of about 0 ∼ 20 GHz probe detuning, namely, as the probe wave is shifted to outside the corresponding detuning region, new conjugate signals cannot be observed. Furthermore, in order to ensure effective FWM interaction, the tunable range of probe detuning illustrated in Fig. 11(a) is remarkably narrower than that in Fig. 3. This behavior can be explained that, after injected probe wave with enough high power is far from the selected side mode, they have no overlap each other in spacing region so that the power of side mode cannot be enhanced by the probe wave, resulting in very low pump power that cannot create effective FWM process. Both output power and conversion efficiency shown in Fig. 11(b) and (c) have similar variation trends to those of Fig. 3(b) and (c), and they have similarly physical mechanisms to induce the behaviors. Here, other noticeable issue is that only positive frequency detuning for probe wave, i.e., injected frequency needs little higher than the referred side mode, may achieve nearly degenerate FWM process attributed to the case that side mode in free-running spectrum has no enough high power level. According to above analysis, one can conclude that, under the condition of injected wave with enough high power level, nearly degenerate FWM interaction can be obtained by judiciously adjusting power and frequency of probe wave while dominant mode or side mode is, respectively, selected as pump wave.

4. Conclusion

In this work, nearly degenerate FWM processes are demonstrated and discussed in SMFP-LD subject to single beam optical injection. In investigation, the dominant mode or residual side mode of free-running spectrum is, respectively, selected as pump wave, and the external injection beam is called as probe wave. Therefore, based on the classical pump-probe structure, nearly degenerate FWM phenomena are exhibited and analyzed with variable probe power, and probe detuning, ranging from −50 GHz to 50 GHz. Higher order conjugate signals resulting from cascade FWM processes are also observed in very small pump-probe detuning. While probe wave is shifted from right to left side of dominant mode, FWM phenomenon can be easily attained by judiciously changing the power and frequency detuning of probe wave. However, in order to produce effective nearly degenerate FWM, the probe wave must be located on high frequency side of side mode as the pump wave because power of the corresponding side mode is too low. Some new signals around other lasing resonance modes with enough high power are also observed. These results in this study will have very outstanding applications in the aspects of optical sensor, low frequency microwave and millimeter wave generation, and so on, which will further be researched in future work.

References

[1] R. Nietzke, P. Fenz, W. Eisasser, and E. O. Gobel, “Cascade four-wave mixing in semiconductor lasers,” *Appl. Phys. Lett.*, vol. 51, no. 17, pp. 1298–1300, Oct. 1987.

[2] H. C. Li, G. Q. Ge, and H. Y. Zhang, “Coexistence of three-wave, four-wave, and five-wave mixing processes in a superconducting artificial atom,” *Opt. Lett.*, vol. 40, no. 6, pp. 1133–1136, Mar. 2015.

[3] I. C. Khoo, "Degenerate four-wave mixing in the nematic phase of a liquid crystal," *Appl. Phys. Lett.*, vol. 38, no. 3, pp. 123–124, Feb. 1981.
[4] S. R. Petersen, T. T. Alkeskjold, C. B. Olausson, and J. Lægsgaard, "Intermodal and cross-polarization four-wave mixing in large-core hybrid photonic crystal fibers," *Opt. Exp.*, vol. 23, no. 5, pp. 5954–5971, Mar. 2015.
[5] C. Karaguleff, G. I. Stegeman, R. Fortenberry, R. Zanoni, and C. T. Seaton, "Degenerate four-wave mixing in planar CS2 covered waveguides," *Appl. Phys. Lett.*, vol. 46, no. 7, pp. 621–623, Apr. 1985.
[6] S. K. Turitsyn, A. E. Bednyakova, M. P. Fedoruk, S. B. Papernyi, and W. R. L. Clements, "Inverse four-wave mixing and self-parametric amplification in optical fibre," *Nat. Photon.*, vol. 9, no. 9, pp. 608–614, Aug. 2015.
[7] F. Morichetti, A. Canciamilla, C. Ferrari, A. Samarelli, M. Sorel, and A. Melloni, "Travelling-wave resonant four-wave mixing breaks the limits of cavity-enhanced all-optical wavelength conversion," *Nat. Commun.*, vol. 2, May 2011, Art. no. 296.
[8] G. Y. Chen, Y. Yu, and X. L. Zhang, "Optical phase erasure and wavelength conversion using silicon nonlinear waveguide with reverse biased PIN junctions," *IEEE Photon. J.*, vol. 7, no. 5, Oct. 2015, Art. no. 7102808.
[9] S. R. Petersen, T. T. Alkeskjold, C. B. Olausson, and J. Lægsgaard, "Polarization switch of four-wave mixing in large mode area hybrid photonic crystal fibers," *Opt. Lett.*, vol. 40, no. 4, pp. 487–490, Feb. 2015.
[10] L. Zhang, T. H. Tuan, H. kawamura, T. Suzuki, and Y. Ohishi, "Optical parametric oscillator based on degenerate four-wave mixing in suspended core tellurite microstructured optical fiber," *Opt. Exp.*, vol. 23, no. 20, pp. 26299–26304, Oct. 2015.
[11] J. Wang, Q. Z. Sun, J. Q. Sun, and X. L. Zhang, "Experimental demonstration on 40 Gbit/s all-optical multicasting logic XOR gate for NRZ-DPSK signals using four-wave mixing in highly nonlinear fiber," *Opt. Commun.* vol. 282, no. 13, 2615–2619, Jul. 2009.
[12] B. Li *et al.*, "All-optical digital logic AND and XOR gates using four-wave-mixing in monolithically integrated semiconductor ring lasers," *Electron. Lett.*, vol. 45, no. 13, pp. 698–700, Jun. 2009.
[13] S. H. Tang, Z. X. Wu, F. Xu, and Y. Q. Lu, "Simulation of optical microfiber strain sensors based on four-wave mixing," *IEEE Sensors J.*, vol. 16, no. 9, pp. 3068–3074, Feb. 2016.
[14] V. Venkataraman, P. Londero, A. R. Bhagwat, A. D. Slepkov, and A. L. Gaeta, "All-optical modulation of four-wave mixing in an Rb-filled photonic bandgap fiber," *Opt. Lett.*, vol. 35, no. 13, pp. 2287–2289, Jul. 2010.
[15] I. V. Babushkin, F. Noack, and J. Herrmann, "Generation of sub-5 FS pulses in vacuum ultraviolet using four-wave frequency mixing in hollow waveguides," *Opt. Lett.*, vol. 33, no. 9, pp. 938–940, May 2008.
[16] P. Kultavewuti, E. Y. Zhu, L. Qian, V. Pusino, M. Sorel, and J. S. Aitchison, "Correlated photon pair generation in AlGaAs nanowaveguides via spontaneous four-wave mixing," *Opt. Exp.*, vol. 24, no. 4, pp. 3365–3376, Feb. 2016.
[17] S. S. Jyu *et al.*, "250-GHz passive harmonic mode-locked Er-doped fiber laser by dissipative four-wave mixing with silicon-based micro-ring," *IEEE Photon. J.*, vol. 5, no. 5, Oct. 2013, Art. no. 1502107.
[18] M. Matsuura, F. Gomez-Agis, N. Calabretta, O. Raz, and H. J. S. Dorren, "320-to-40-Gb/s optical demultiplexing using four-wave mixing in a quantum-dot SOA," *IEEE Photon. Technol. Lett.*, vol. 24, no. 2, pp. 101–103, Oct. 2011.
[19] H. Huang, K. Schires, P. J. Poole, and F. Grillot, "Non-degenerate four-wave mixing in an optically injection-locked InAs/InP quantum dot Fabry-Perot laser," *Appl. Phys. Lett.*, vol. 106, Apr. 2015, Art. no. 143501.
[20] T. Sadeev, H. Huang, D. Arsenijević, K. Schires, F. Grillot, and D. Bimberg, "Highly efficient non-degenerate four-wave mixing under dual-mode injection in InP/InAs quantum-dash and quantum-dot lasers at 1.55 μm," *Appl. Phys. Lett.*, vol. 107, Nov. 2015, Art. no. 191111.
[21] S. M. Gao, E. K. Tien, Q. Song, Y. W. Huang, and O. Boyraz, "Ultra-broadband one-to-two wavelength conversion using low-phase-mismatching four-wave mixing in silicon waveguides," *Opt. Exp.*, vol. 18, no. 11, pp. 11898–11903, May 2010.
[22] H. Zhou *et al.*, "Enhanced four-wave mixing n grapheme-silicon slow-light photonic crystal waveguides," *Appl. Phys. Lett.*, vol. 105, Sep. 2014, Art. no. 091111.
[23] A. Anchal, K. P. Kumar, S. O'Duill, and P. M. Anandarajah, "Experimental demonstration of optical phase conjugation using counter-propagating dual pumped four-wave mixing in semiconductor optical amplifier," *Opt. Commun.*, vol. 369, pp. 106–110, Feb. 2016.
[24] P. Friedli *et al.*, "Four-wave mixing in a quantum cascade laser amplifier," *Appl. Phys. Lett.*, vol. 102, Jun. 2013, Art. no. 222104.
[25] Y. H. Ding, J. Xu, H. Y. Qu, and C. Peucheret, "Mode-selective wavelength conversion based on four-wave mixing in a multimode silicon waveguide," *Opt. Exp.*, vol. 22, no. 1, pp. 127–135, Dec. 2013.
[26] A. Hurtado, R. Raghunathan, I. D. Henning, M. J. Adams, and L. F. Lester, "Simultaneous microwave- and millimeter-wave signal generation with a 1310-nm quantum-dot-distributed feedback laser," *IEEE J. Sel. Topics Quantum Electron.*, vol. 21, no. 6, Nov./Dec. 2015, Art. no. 1801207.
[27] Y. D. Jeong, Y. H. Won, S. O. Choi, and J. H. Yoon, "Tunable single-mode Fabry-Pérot laser diode using a built-in external cavity and its modulation characteristics," *Opt. Lett.*, vol. 31, no. 17, pp. 2586–2588, Sep. 2006
[28] H. Wu, N. H. Zhu, J. W. Man, and H. Q. Yuan, "Continuously wavelength-tunable laser source using a self-injected Fabry-Pérot laser diode," *IEEE Photon. Technol. Lett.*, vol. 23, no. 6, pp. 332–334, Mar. 2011.
[29] M. R. Uddin and Y. H. Won, "All-optical wavelength conversion by the modulation of self-locking state of a single-mode FP-LD," *IEEE Photon. Technol. Lett.*, vol. 22, no. 5, pp. 290–292, Mar. 2010.
[30] J. W. Wu and Y. H. Won, "Temporal response of optical intensity modulation based on side-mode injection locked single-mode Fabry-Pérot laser diode," *J. Opt.-UK*, vol. 15, no. 7, Jul. 2013, Art. no. 075502.
[31] J. W. Wu, B. Nakarmi, Q. H. Tran, and Y. H. Won, "Influence of wavelength detuning on the optical logic gate in side-mode injection locked single-mode Fabry-Pérot laser diode," *Opt. Commun.*, vol. 294, pp. 233–236, May 2013.
[32] J. W. Wu, B. Nakarmi, and Y. H. Won, "Optically tunable microwave, millimeter-wave and submillimeter-wave utilizing single-mode Fabry-Perot laser diode subject to optical feedback," *Opt. Exp.*, vol. 24, no. 3, pp. 2655–2663, Jan. 2016.
[33] N. L. Hoang, J. S. Cho, Y. H. Won, and Y. D. Jeong, "All-optical flip-flop with high on-off contrast ratio using two injection-locked single-mode Fabry-pérot laser diodes," *Opt. Exp.*, vol. 15, no. 8, pp. 5166–5171, Apr. 2007.

[34] J. W. Wu, B. Nakarmi, and Y. H. Won, "Highly nondegenerate four-wave mixing in single-mode Fabry–Perot laser diode subject to dual-mode injection," *IEEE Photon. J.*, vol. 8, no. 2, Apr. 2016, Art. no. 6100210.
[35] S. J. Jiang and M. Dagenais, "Nearly degenerate four-wave mixing in Fabry-Perot semiconductor lasers," *Opt. Lett.*, vol. 18, no. 6, pp. 1337–1339, Aug. 1993.
[36] T. B. Simpson, J. M. Liu, K. F. Huang, and K. Tai, "Nonlinear dynamics induced by external optical injection in semiconductor lasers," *Quantum Semiclass. Opt.*, vol. 9, pp. 765–784, 1997.
[37] K. Inoue, T. Mukai, and T. Saitoh, "Nearly degenerate four-wave mixing in a traveling-wave semiconductor laser amplifier," *Appl. Phys. Lett.*, vol. 51, no. 14, pp. 1051–1053, Oct. 1987.
[38] F. Surre, B. Kennedy, P. Landais, S. Philippe, and A. L. Bradley, "Polarization resolved four-wave-mixing-based measurement in bulk material semiconductor optical amplifier," in *Proc. Int. Conf. Transparent Opt. Netw.*, 2006, pp. 169–172.
[39] A. Uskov, J. Mørk, and J. Mark, "Wave mixing in semiconductor laser amplifiers due to carrier heating and spectral-hole burning," *IEEE J. Quantum Electron.*, vol. 30, no. 8, pp. 1769–1781, Aug. 1994.
[40] J. Minch, C. S. Chang, and S. L. Chuang, "Four-wave mixing in a distributed-feedback laser," *Appl. Phys. Lett.*, vol. 70, no. 11, pp. 1360–1362, Mar. 1997.
[41] Y. Lefevre, N. Vermeulen, and H. Thienpont, "Simultaneous quasi-phase matching of two arbitrary four-wave-mixing processes," *IEEE J. Lightw. Technol.*, vol. 33, no. 9, pp. 1726–1736, May 2015.
[42] Z. G. Lu *et al.*, "Highly efficient non-degenerate four-wave mixing process in InAs/InGaAsP quantum dots," *Electron. Lett.*, vol. 42, no. 19, pp. 1112–1113, Sep. 2006.
[43] H. Kuwatsuka, H. Shoji, M. Matsuda, and H. Ishikawa, "Nondegenerate four-wave mixing in a long-cavity $\lambda/4$-shifted DFB laser using its lasing beam as pump beams," *IEEE J. Quantum Electron.*, vol. 33, no. 11, pp. 2002–2010, Nov. 1997.
[44] J. P. Donnelly, H. Q. Le, E. A. Swanson, S. H. Groves, A. Darwish, and E. P. Ippen, "Nondegenerate four-wave mixing wavelength conversion in low-loss passive InGaAsP-InP quantum-well waveguides," *IEEE Photon. Technol. Lett.*, vol. 8, no. 5, pp. 2623–625, May 1996.